3D printing of biomimetic microstructures for cancer cell migration

Tina Qing Huang · Xin Qu · Justin Liu · Shaochen Chen

Abstract To understand the physical behavior and migration of cancer cells, a 3D *in vitro* micro-chip in hydrogel was created using 3D projection printing. The micro-chip has a honeycomb branched structure, aiming to mimic 3D vascular morphology to test, monitor, and analyze differences in the behavior of cancer cells (i.e. HeLa) vs. non-cancerous cell lines (i.e. 10 T1/2). The 3D Projection Printing system can fabricate complex structures in seconds from user-created designs. The fabricated microstructures have three different channel widths of 25, 45, and 120 microns wide to reflect a range of blood vessel diameters. HeLa and 10 T1/2 cells seeded within the micro-chip were then analyzed for morphology and cell migration speed. 10 T1/2 cells exhibited greater changes in morphology due to channel size width than HeLa cells; however, channel width had a limited effect on 10 T1/2 cell migration while HeLa cancer cell migration increased as channel width decreased. This physiologically relevant 3D cancer tissue model has the potential to be a powerful tool for future drug discoveries and cancer migration studies

Keywords 3D printing · Cancer cell migration · Microchip · Hydrogel

1 Introduction

Metastasis is a complex chain of events by which cancer cells leave an original tumor site and migrate to other areas of the body either through the circulatory or lymphatic system. (Lauffenburger and Horwitz 1996), (Steeg 2006) Once cancer has reached a metastasizing stage, the probability that patients will survive for more than a year is less than 50 %. (Decaestecker et al. 2007) Some cancers, such as glioblastomas, arise from dramatic migration. To understand metastasis, we need to understand how cancer cells migrate. The development of future methods to treat and target cancer requires determining the various factors that affect cell migration. In addition, current drug testing in two-dimensional (2D) culture can be aided by designing a more accurate 3D cancer tissue model.

To design a more accurate model, some studies have studied migration *in vivo*. Leong et. al. used the chick embryo's thin chorioallantoic membrane (CAM) combined with fluorescently labeled cancer cells to study cancer migration *in vivo*. (Leong et al. 2012) In other studies, transgenic mice were used to mimic the process of breast cancer metastasis. (Jenkinson et al. 2004) However, while the mouse model mirrored the human process, the time required to grow metastasized tumors and the high cost associated with maintaining the mice detracted from the effectiveness of such a model. (Zhou et al. 2011) Recently, *in vitro* models have been developed to investigate metastasis. (Jenkinson et al. 2004),(Yamada and Cukierman 2007),(Watson et al. 1995) 2D *in vitro* migration studies have used approaches such as microcarrier bead assays as well as a monolayer wound model. (Decaestecker et al. 2007), (Ghajar et al. 2007), (Mathew et al. 1997), (Chaffer et al. 2006) In addition, single-cell locomotion assays have proven useful in separating cell migration from cell growth. (Decaestecker et al. 2007), (Albrecht-Buehler 1977) Recent studies on 3D *in vitro* migration systems provide more understanding of cell migration. (Rolli et al. 2010), (Mak et al. 2011), (Pathak and Kumar 2012) One such model by Heuze et al. used linear polydimethylsiloxane (PDMS) channels to analyze how channel width and shape affect migration speed. (Heuzé et al. 2011) In a different study, linear channels, with "high" tapered angles or "low" tapered angles, were used to

T. Q. Huang · X. Qu · S. Chen (✉)
Department of NanoEngineering, University of California, MC-0448, SME Building 245B, 9500 Gilman Drive, La Jolla, San Diego, CA 92093, USA
e-mail: chen168@eng.ucsd.edu

J. Liu
Department of Materials Science and Engineering, University of California, MC-0448, SME Building 245B, 9500 Gilman Drive, La Jolla, San Diego, CA 92093, USA

study migratory response of cells to physical spatial gradients. (Mak et al. 2011) Their findings suggested a feedback mechanism that pushes metastatic cancer cells into increased aggressiveness when invading even more confined spaces. Similarly, an additional study indicated cancer cell's migration speed decreased with increasing channel width (Irimia and Toner 2009; Mathew et al. 1997).

In this work, we utilized a novel microfabrication technique to create a biomimetic 3D microstructure to further understand cancer migration. 3D bioprinting is an emerging field that deserves further implementation. Different forms of maskless fabrication, such as scanning polymerization and projection polymerization, are capable of creating detailed microstructures. One recently developed projection writing technology, called Digital Micromirror Device-based Projection Printing (DMD-PP), can fabricate microscale three-dimensional structures out of soft and biocompatible hydrogels. (Lu and Chen 2008), (Grogan et al. 2013), (Suri et al. 2011), (Soman et al. 2012c), (Gauvin et al. 2012), (Fozdar et al. 2011), (Soman et al. 2012b), (Han et al. 2010), (Zhang et al. 2012) Using an array of digitally controlled micromirrors, the DMD-PP system projects user-defined images onto a photopolymerizable prepolymer solution to form 3D scaffolds. (Grogan et al. 2013) The DMD-PP system we used in this study is a non-contact fabrication scheme that is capable of fabricating detailed and intricate geometries within seconds, which gives it an advantage over other methods of fabrication. For example, microcontact printing and photolithography methods are time intensive and 2D in nature with multistep processes that require extensive instrumentation. Some of these processes are not compatible with cells and biological materials. Compared to the conventional PDMS based platforms(Mak et al. 2011), (Balaban et al. 2001), (Vedula et al. 2012), which has an elastic modulus of approximately 1 MPa, our biomaterial has greater flexibility in tuning microstructure stiffness. (Brown et al. 2005) In addition, the versatility of the DMD-PP process allows rapid alterations of scaffold mechanical properties by altering the composition of the prepolymer solution. The DMD-PP method allows one to create 3D, biomimetic scaffolds in biomaterials with varying pattern design.

2 Experiment

2.1 Materials and fabrication using the DMD-PP printing system

As described previously, the DMD-PP method was used to fabricate the microstructures (Fig. 1). (Lu and Chen 2008), (Grogan et al. 2013), (Suri et al. 2011), (Soman et al. 2012c), (Gauvin et al. 2012), (Fozdar et al. 2011), (Soman et al. 2012b), (Han et al. 2010), (Zhang et al. 2012) In brief, user-created branched honeycomb design was loaded into the

computer, and the digital light processing chip projected the design down to the prepolymer solution with a uniform UV light. (Soman et al. 2012a) Prior to successful fabrication, polymer solution and test conditions were optimized, including the stage coordinates and UV exposure time for polymerization. Underexposure or overexposure to UV light would cause the structure to either not be fully formed or over-polymerized. Different channel widths were fabricated using different UV exposure times: 25, 45, and 120 μm channels required 1.25 s, 1.5 s, and 4.5 s of UV exposure, respectively. After polymerization, each structure was rinsed with Dulbecco's Phosphate Buffered Saline to remove any remaining unpolymerized solution and prepared for cell culture.

Poly (ethylene glycol) diacrylate (PEGDA, MW=700, Sigma) was chosen as the microstructure material because of its high water content, biocompatibility, and tunable mechanical properties. (Ifkovits and Burdick 2007), (Nguyen and West 2002) PEGDA material can also be conjugated with several signaling molecules for modulating cell growth and function. Lithium phenyl-2,4,6-trimethylbenzoylphosphinate (LAP) was used as a photo-initiator. Tempo (Sigma) was used to absorb free radical production and optimize the resolution at the feature plane. 5-Benzoyl-4-hydroxy-2-methoxybenzenesulfonic acid (HMBS, Sigma) was used to optimize the resolution at the planes above and below the feature plane. This 3D bioprinter fabricated the microstructures using selective UV polymerization of a 20 % PEGDA+1 % LAP+0.01 % Tempo+0.1 % HMBS solution.

2.2 Cell culture

Murine 10 T1/2 cells were purchased from ATCC and cultured according to the protocol provided by vendor using Dulbecco's Modified Eagle Medium Growth Media (Gibco) and 10 % Fetal Bovine Serum (FBS) (HyClone). HeLa cells were a generous gift from Professor Shu Chien's group at the University of California, San Diego. They were cultured using the same media as the 10 T1/2 cells. All experiments were carried out using cells from passage 2 to passage 5. Cells were harvested and counted based on the general protocol and then seeded onto the microstructure with growth media. The cultures were maintained in a 37 °C incubator with 5 % CO_2.

2.3 Experimental setup

Two cell lines, 10 T1/2 and HeLa, were utilized. Cells were seeded in parallel on separate 25, 45, and 120-μm-channel-wide structures. Cells were imaged on scaffolds using a Leica DMI6000 B microscope for time lapse imaging at different time points. Two key sets of data were extracted: cell area and cell migration speed. Fiji, an open-source distribution of ImageJ was used to extract that data from the images taken. Time lapsed images were aligned, tracked, and analyzed.
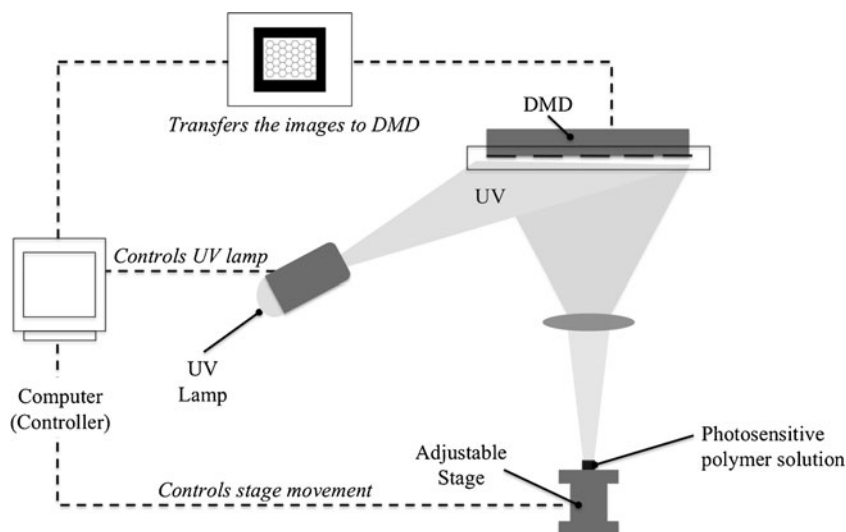
Instantaneous velocity was calculated by dividing distance travelled from one time frame to the next by the time lapsed.

2.4 Statistical analysis

Data are reported as mean ± standard error of the mean. Comparison of sample means was performed by ANOVA followed by Tukey's post-hoc test (SPSS software), $p < 0.05$.

3 Results and discussion

Three different sets of microstructures were used in this study: branched honeycomb design with 25, 45, and 120-μm-wide channels. HeLa and 10 T1/2 cells were seeded on separate but identical structures and the resulting time-lapsed images were analyzed using Fiji scientific image analysis software.

3.1 Microstructure design

The DMD-PP biofabrication system can create intricate scaffolds. Using this capability, we successfully fabricated a 3D replica of a capillary structure in seconds. We converted images of rat capillaries into a 3D model and fabricated it using a 100 % 700 MW PEGDA prepolymer solution. The versatility of the DMD-PP platform allows the user to vary channel widths while changing focal planes within continuous exposure, producing a refined vascular structure, as seen in Fig. 2. The resulting 3D scaffold was an exact replica of the real image in terms of morphology. However, due to the complex nature of the vascular structure, any cell studies conducted on the printed vasculature would be extremely difficult to analyze. Since channels have a large range of widths (10 to 150 μm), altered curvature angles, and directionality angles, it would be complicated to correlate migration speed and morphology data to one variable.

Previous studies used strictly linear or tapered designs to investigate the effects of channel width; however, these patterns do not properly mimic vasculature within the human body. (Mak et al. 2011), (Pathak and Kumar 2012), (Jeon et al. 2010) We created simplified biomimetic honeycomb scaffold, giving us control over channel width, while still preserving the branched capillary structure. Simplifying the structure allows for the independent regulation and analysis of channel width on migration speed and cell morphology. Following fabrication, image analysis software was used to measure channel widths. We chose channel widths of 25, 45, and 120 μm to reflect varying diameters of blood vessels, ranging from capillaries to small arteries. (Wiedeman 1963) As seen in Fig. 3, the final fabricated scaffolds (Fig. 3b) show great consistency with the original design (Fig. 3a). Cells were seeded on the fabricated microstructures of all three designs, and within the timeframe of our experiment, cells migrated only within the
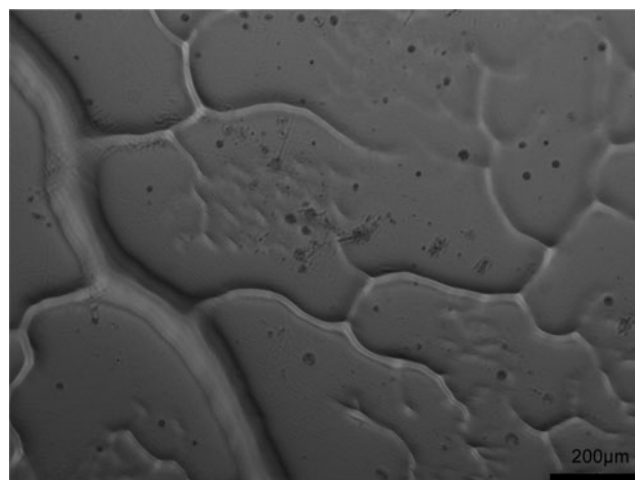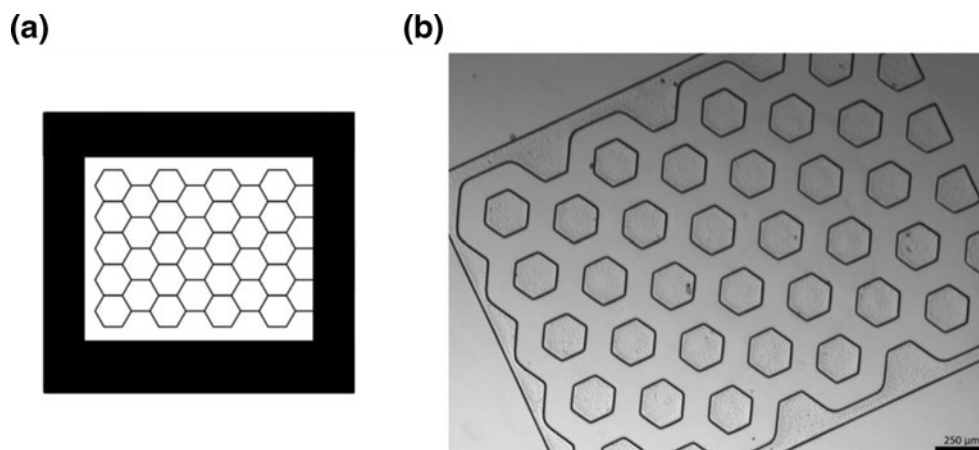

Fig. 2 Image of a 3D printed microscaffold. A real microCT scan of rat capillaries was converted into a 3D model and printed using the DMD-PP system

channels and did not grow onto the hexagonal platforms (Fig. 4).

3.2 Cell Morphology analysis

Statistical analysis was performed in order to further understand the significance of the findings relating 10 T1/2 and HeLa cell shape to channel microstructure. The average cell area of 10 T1/2 and HeLa cells (Fig. 5) in the 25 μm, 45 μm, and 120 μm channels were compared. The HeLa cell area was observed to be significantly larger in 25 μm channels when compared to both 45 and 120 μm channels ($p < 0.05$). Specifically, the 10 % decrease in cell area from 25 to 120 μm channels may be explained by the flexibility of cancerous cells during migration. (Wirtz et al. 2011) Because HeLa cells migrated fastest in 25 μm channels, cells may have undergone additional spreading, increasing their area. By comparison, 10 T1/2 cells were not as affected by channel width as HeLa cells. 10 T1/2 cell area in 120 μm channels was significantly larger compared to both 25 and 45 μm channels ($p < 0.05$). This may be because narrower channels potentially led to increased cell-cell communication and interaction. (Jeon et al. 2010) In addition, other studies have shown that fibroblast cells seeded in narrow strips had increased alignment and directionality. (Jeon et al. 2010), (Li et al. 2001) This was an

additional indication that geometric cues can influence aspects of cell behavior.

3.3 Migration speed analysis

Time lapse microscopy was used to assess cell migration. Interestingly, cells were observed to migrate at different speeds depending on the channel width of each structure. As seen in Fig. 5a, as the channel width increased, the migration speed of the HeLa cells decreased. From 25 to 45 to 120 μm wide channels, the speeds decreased from 14 to 9 to 6 μm/h, respectively. However, the migration speed of 10 T1/2 cells was not affected by the channel width (Fig. 6).

These results are consistent with the *in vivo* understanding of cancer metastasis, which shows that cancer cells must alter their morphology and other physical interactions in order to achieve intravasation. (Pathak and Kumar 2012), (Gupta and Massagué 2006; Takeda et al. 2002) Therefore, because cancer cells migrate through variously-wide blood vessels in order to spread beyond the primary tumor, blood vessel diameter affects cancer cell migration speed. This process of cancer metastasis also explains why HeLa cells migrated with the greatest velocity in the narrowest channels in our experiments: narrow channels promote cell polarization and therefore enhance the migration speed. (Pathak and Kumar 2012) These
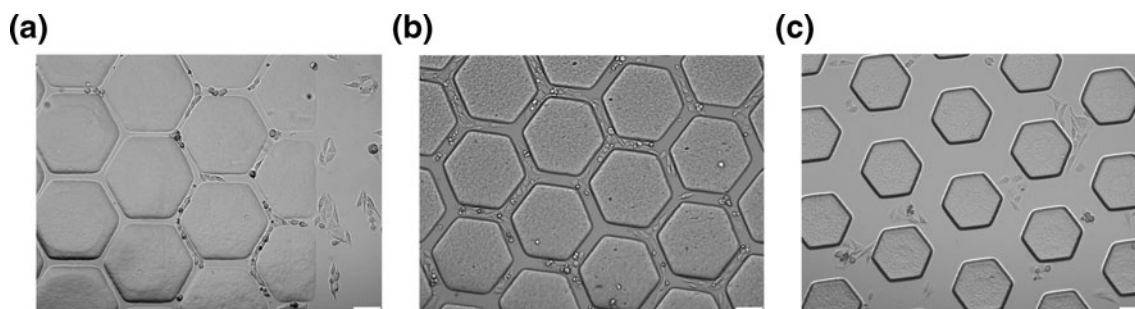

Fig. 4 Optical microscope images of HeLa cells seeded on fabricated PEGDA microstructures with (**a**) 25-μm-wide channels, (**b**) 45-μm-wide channels, and (**c**) 120-μm-wide channels. Each error bar represents 100 μm
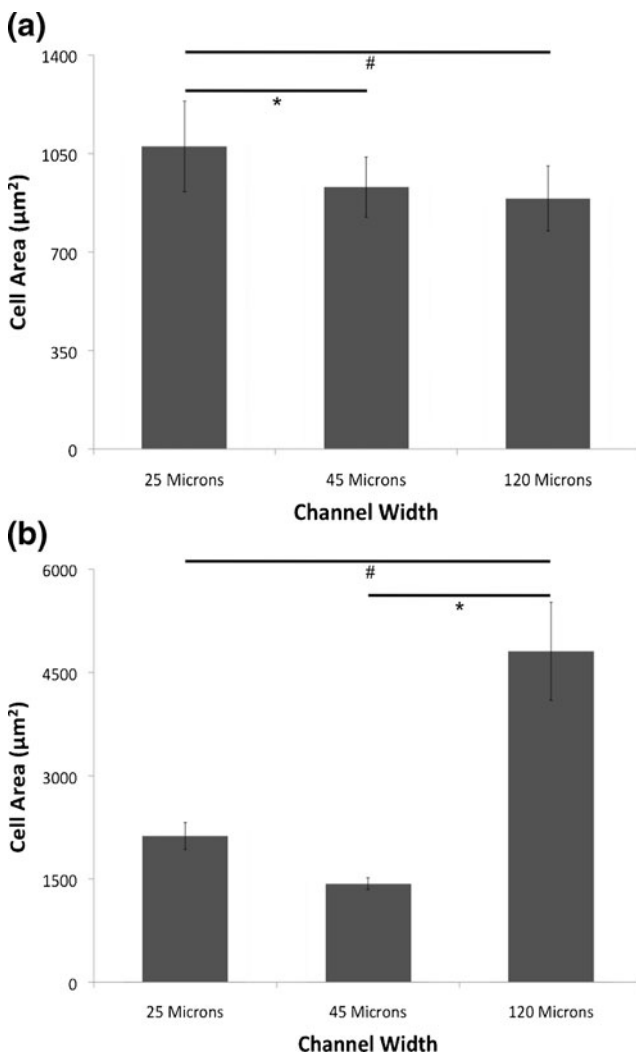
Fig. 5 Area of (a) HeLa and (b) 10 T1/2 cells on microstructures of 25, 45, and 120 μm wide channels. Statistically different pairs (p <0.05) are indicated by horizontal lines and either # or *

Fig. 6 Graphs showing the average instantaneous speed of (a) HeLa and (b) 10 T½ cells cultured on microstructures. Statistically different pairs (p <0.05) are indicated by horizontal lines and #

results are also consistent with the angiogenesis model in cancer progression (Steeg 2006; Zetter 1998).

However, while our data showed that channel width changes affected HeLa cells, 10 T½ cells were not significantly affected. For each type of channel width, the cell migration speed was statistically similar. This could be explained by the nature of the 10 T½ cell locomotion, which might be less sensitive to geometric cues. Cancerous and noncancerous cell responses to geometric cues are interesting because the mechanisms behind those differences may be potential strategy for cancer treatment.

4 Conclusions

In this study, we demonstrated the effects of geometric cues on 10 T1/2 and HeLa cells using a biomimetic micro-chip fabricated by 3D projection printing. The honeycomb design of the
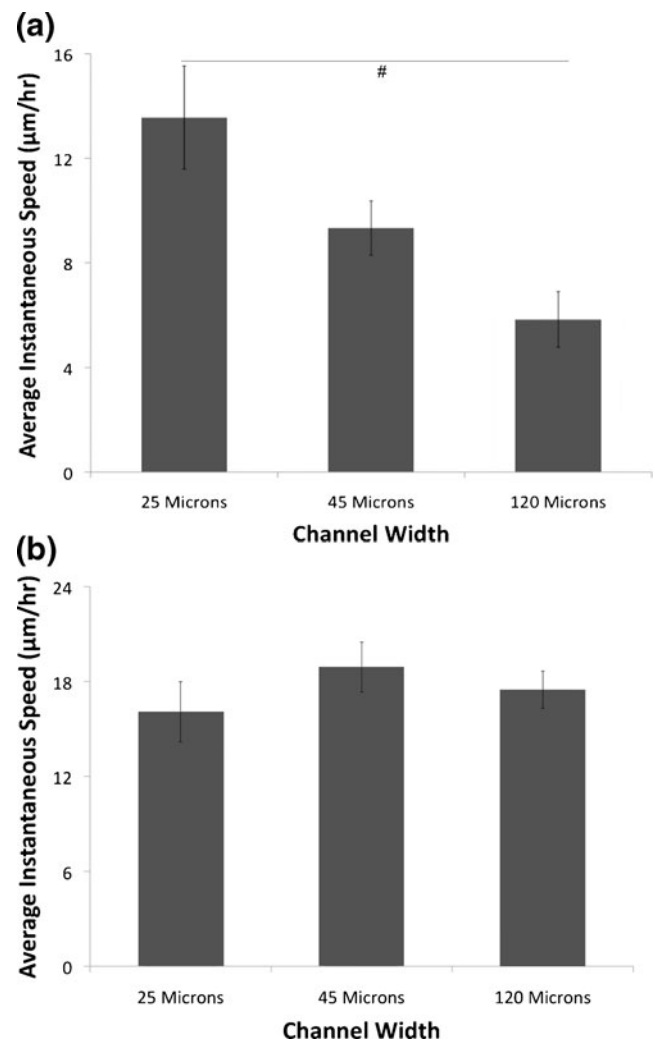
micro-chip mimics the structure of human blood vessels, which allows for results with physiological relevance. Our results indicate that HeLa cell area and migration speed was affected by geometric cues, with decreased cell area corresponding with increased cell migration speed. These results may further indicate that cancer cell metastasis and aggressiveness is affected by vessel size. (Gallego-Perez et al. 2012) In contrast, 10 T1/2 cell migration speed was not significantly influenced by channel size. The different responses between 102 T1/2 and HeLa cells to geometric cues could lead to a better strategy to investigate cancer biology as well as metastasis.

Future cell studies may explore the differences in normal and cancerous cell responses to geometry to test antimigratory cancer drugs in this micro-chip. There is also the potential to utilize the DMD-PP system to encapsulate different cell types, simulating cancer cell invasion of various tissue targets. This would allow for more biomimetic results when conducting migration studies, drug screening tests, or other cell studies

within the structures. This work represents a significant step forward in our ability to create a rapid and cost-efficient physiologically relevant 3D cancer tissue model, providing a powerful tool for investigating cancer migration.

References

G. Albrecht-Buehler, Cell **11**, 395 (1977)

N.Q. Balaban, U.S. Schwarz, D. Riveline, P. Goichberg, G. Tzur, I. Sabanay, D. Mahalu, S. Safran, A. Bershadsky, L. Addadi, B. Geiger, Nat. Cell Biol. **3**, 466 (2001)

X.Q. Brown, K. Ookawa, J.Y. Wong, Biomaterials **26**, 3123 (2005)

C.L. Chaffer, J.P. Brennan, J.L. Slavin, T. Blick, E.W. Thompson, E.D. Williams, Cancer Res. **66**, 11271 (2006)

C. Decaestecker, O. Debeir, P. Van Ham, R. Kiss, Med. Res. Rev. **27**, 149 (2007)

D.Y. Fozdar, P. Soman, J.W. Lee, L.-H. Han, S. Chen, Adv. Funct. Mater. **21**, 2712 (2011)

D. Gallego-Perez, N. Higuita-Castro, L. Denning, J. DeJesus, K. Dahl, A. Sarkar, D.J. Hansford, Lab Chip **12**, 4424 (2012)

R. Gauvin, Y.-C. Chen, J.W. Lee, P. Soman, P. Zorlutuna, J.W. Nichol, H. Bae, S. Chen, A. Khademhosseini, Biomaterials **33**, 3824 (2012)

C.M. Ghajar, V. Suresh, S.R. Peyton, C.B. Raub, F.L. Meyskens, S.C. George, A.J. Putnam, Mol. Cancer Ther. **6**, 552 (2007)

S.P. Grogan, P.H. Chung, P. Soman, P. Chen, M.K. Lotz, S. Chen, D.D. D'Lima, Acta Biomater. **9**, 7218 (2013)

G.P. Gupta, J. Massagué, Cell **127**, 679 (2006)

L.-H. Han, S. Suri, C.E. Schmidt, S. Chen, Biomed. Microdevices **12**, 721 (2010)

M. Heuzé, O. Collin, E. Terriac, Cell Migration **769**, 415 (2011)

J.L. Ifkovits, J.A. Burdick, Tissue Eng. **13**, 2369 (2007)

D. Irimia, M. Toner, Integr. Biol. **1**, 506 (2009)

S.R. Jenkinson, R. Barraclough, C.R. West, P.S. Rudland, Br. J. Cancer **90**, 253 (2004)

H. Jeon, H. Hidai, D.J. Hwang, K.E. Healy, C.P. Grigoropoulos, Biomaterials **31**, 4286 (2010)

D.A. Lauffenburger, A.F. Horwitz, Cell **84**, 359 (1996)

H.S. Leong, A.F. Chambers, J.D. Lewis, Methods Mol. Biol. **872**, 1 (2012)

S. Li, S. Bhatia, Y.-L. Hu, Y.-T. Shiu, Y.-S. Li, S. Usami, S. Chien, Biorheology **38**, 101 (2001)

Y. Lu, S. Chen, Appl. Phys. Lett. **92**, 041109 (2008)

M. Mak, C.A. Reinhart-King, D. Erickson, PloS ONE **6**, e20825 (2011)

A.C. Mathew, T.T. Rajah, G.M. Hurt, S.M. Abbas Abidi, J.J. Dmytryk, J.T. Pento, Clin & Exper Metast **15**, 393 (1997)

K.T. Nguyen, J.L. West, Biomaterials **23**, 4307 (2002)

A. Pathak, S. Kumar, Proc. Natl. Acad. Sci. U. S. A. **109**, 10334 (2012)

C.G. Rolli, T. Seufferlein, R. Kemkemer, J.P. Spatz, PloS ONE **5**, e8726 (2010)

P. Soman, J.A. Kelber, J.W. Lee, T.N. Wright, K.S. Vecchio, R.L. Klemke, S. Chen, Biomaterials **33**, 7064 (2012a)

P. Soman, J.W. Lee, A. Phadke, S. Varghese, S. Chen, Acta Biomater. **8**, 2587 (2012b)

P. Soman, B.T.D. Tobe, J.W. Lee, A.A.M. Winquist, I. Singec, K.S. Vecchio, E.Y. Snyder, S. Chen, Biomed. Microdevices **14**, 829 (2012c)

P.S. Steeg, Nat. Med. **12**, 895 (2006)

S. Suri, L.-H. Han, W. Zhang, A. Singh, S. Chen, C.E. Schmidt, Biomed. Microdevices **13**, 983 (2011)

A. Takeda, O. Stoeltzing, S.A. Ahmad, N. Reinmuth, W. Liu, A. Parikh, F. Fan, M. Akagi, L.M. Ellis, Ann. Surg. Oncol. **9**, 610 (2002)

S.R.K. Vedula, M.C. Leong, T.L. Lai, P. Hersen, A.J. Kabla, C.T. Lim, B. Ladoux, Proc. Natl. Acad. Sci. U. S. A. **109**, 12974 (2012)

S. A. Watson, T. M. Morris, G. Robinson, B.- Two, H. Colon, C. Metastasis, M. J. Crimmin, P. D. Brown, and J. D. Hardcastle, Cancer Research 3629 (1995)

M.P. Wiedeman, Circ. Res. **12**, 375 (1963)

D. Wirtz, K. Konstantopoulos, P.C. Searson, Nat. Rev. Cancer **11**, 512 (2011)

K.M. Yamada, E. Cukierman, Cell **130**, 601 (2007)

B.R. Zetter, Annu. Rev. Med. **49**, 407 (1998)

A.P. Zhang, X. Qu, P. Soman, K.C. Hribar, J.W. Lee, S. Chen, S. He, Adv. Mater. **24**, 4266 (2012)

Z.N. Zhou, P.J. Boimel, J.E. Segall, Drug Disc Today Disease Mod **8**, 95 (2011)